64-9

ASD-TDR-62-833
Part II

INVESTIGATION OF THE PARA-ORTHO SHIFT OF HYDROGEN

TECHNICAL DOCUMENTARY REPORT NO. ASD-TDR-62-833, PART II
OCTOBER, 1963

AF Aero-Propulsion Laboratory
Research and Technology Division
Air Force Systems Command
Wright-Patterson Air Force Base, Ohio

Project No. 3048, Task No. 30193

(Prepared under Contract No. AF 33(616)-7506 by Air Products and Chemicals, Inc., Allentown, Pennsylvania; R. G. Clark, J. F. Kucirka, A. Jambhekar, and G. E. Schmauch (Project Leader), authors.)

ASD-TDR-62-833
Part II

INVESTIGATION OF THE PARA-ORTHO SHIFT OF HYDROGEN

TECHNICAL DOCUMENTARY REPORT NO.
ASD-TDR 62-833, Part II
October 1963

AF Aero-Propulsion Laboratory
Research and Technology Division
Air Force Systems Command
Wright-Patterson Air Force Base, Ohio

Project No. 3048, Task No. 30193

(Prepared under Contract No. AF33(616)-7506 by Air Products and Chemicals, Inc., Allentown, Pennsylvania; R. G. Clark, J. F. Kucirka, A. Jambhekar, and G. E. Schmauch (Project Leader), Authors)

Air Products and Chemicals INC.

NOTICES

When Government drawings, specifications, or other data are used for any purpose other than in connection with a definitely related Government procurement operation, the United States Government thereby incurs no responsibility nor any obligation whatsoever; and the fact that the Government may have formulated, furnished, or in any way supplied the said drawings, specifications, or other data, is not to be regarded by implication or otherwise as in any manner licensing the holder or any other person or corporation, or conveying any rights or permission to manufacture, use, or sell any patented invention that may in any way be related thereto.

Qualified requesters may obtain copies of this report from the Defense Documentation Center (DDC), (formerly ASTIA), Cameron Station, Bldg. 5, 5010 Duke Street, Alexandria 4, Virginia.

This report has been released to the Office of Technical Services, U. S. Department of Commerce, Washington 25, D.C., for sale to the general public.

Copies of this report should not be returned to the Aeronautical Systems Division unless return is required by security considerations, contractual obligations, or notice on a specific document.

Air Products and Chemicals INC.

FOREWORD

This report was prepared by Air Products and Chemicals, Inc., under USAF Contract No. AF33(616)-7506. This contract was initiated under Project No. 3048, "Aviation Fuels", Task No. 30193, "High Energy Fuels". This work begun under the direction of the Directorate of Materials and Processes, Aeronautical Systems Division, Wright-Patterson Air Force Base, Ohio, with Messrs. James H. L. Lawler and Perie R. Pitts, Jr. acting as project engineers. This report will be administered under the direction of the Technical Support Division, Air Force Aero Propulsion Laboratory, Research and Technology Division.

This final report covers work conducted from March 1962 to September 1962 and includes the technical information contained in Quarterly Progress Report VII.

The work discussed in this report was supervised by Mr. J. A. Carlson, Jr., Manager of Advanced Projects, and was directed by Dr. Clyde McKinley, Director, Research and Development Department. Special thanks are due Mr. H. E. Lindenmoyer, Mr. L. Cirocco and Mr. S. W. Shurskis for their contributions to the experimental programs. The authors express their gratitude to Mr. G. M. Gigliotti, for his technical editorship and Miss M. Frederick for preparing the manuscript.

This report is Part II of a three-part report which includes Part I, II, and a classified supplement.

ABSTRACT

Investigations of the low-temperature, heterogeneous catalysis of the para-ortho shift of hydrogen for the recovery of the endothermic heat of conversion as low-temperature refrigeration are reported. The research program included: studies of the effects of catalyst activation temperature, particle size, and chamber diameter on conversion activity; adsorption studies; the determination of separation factors of advanced catalysts; and preliminary work to determine the magnetic properties of advanced catalysts.

An extensive catalyst development program has resulted in improved catalyst systems for the conversion. The most advanced catalyst shows an activity 10.5 times more effective, on a weight basis, than hydrous ferric oxide gel which is the best commercial catalyst available for the conversion.

This technical documentary report has been reviewed and is approved.

Marc P. Dunnam
MARC P. DUNNAM
Chief, Technical Support Division
AF Aero Propulsion Laboratory

Part II of Final Report

TABLE OF CONTENTS

LIST OF TABLES

I. INTRODUCTION

With the increasing interest in the use of hydrogen as an air breathing engine propellant, the originators of PR No. 08189 have recognized the intriguing possibilities of recovering the refrigeration from vaporizing liquid parahydrogen. It is known that molecular hydrogen exists in two modifications, which are designated as orthohydrogen and parahydrogen. An equilibrium, which is a function of temperature, exists between these two forms. Under equilibrium conditions, the parahydrogen concentration varies from essentially 100% para at 20° K and below, to approximately 25% para at 150° K and above.

Since the para to orthohydrogen conversion is endothermic in the temperature range of 20° K to 150° K, certain additional low temperature refrigeration is available if the hydrogen is at or near equilibrium at all temperatures along a heat exchanger. In order to recover this low temperature conversion refrigeration, extremely high conversion rates must be achieved. Therefore, the objectives of this investigation were the determination of the parameters that effect this shift of para-to orthohydrogen and the development of a method for speeding the shift toward the equilibrium ratio at low temperatures. These objectives were accomplished through a catalyst development program which ultimately resulted in a catalyst 10.5 times more effective than the best commercial catalyst for this reaction.

Manuscript released by authors June 1963 for publication as an ASD Technical Documentary Report.

II. CATALYST DEVELOPMENT PROGRAM

Low-temperature, heterogeneous catalysis is considered the most promising technique for effecting the para-orthohydrogen conversion at the rate and under the conditions specified in the existing contract. The catalytic effect is attributed to the influence of the inhomogeneous magnetic field of the magnetic component of the catalyst upon the physically adsorbed hydrogen. Therefore, the primary requirements for an effective catalyst are considered to be high physical adsorptive capacity for hydrogen, or high surface area, high concentration of magnetic component in the catalyst and a magnetic component in the catalyst with a high magnetic moment.

The preparation and testing of improved catalyst materials continued during the final months of the contract period. Much of the effort was concentrated on the catalyst system which was under study for the last several reporting periods. Several novel starting materials and complex preparation techniques were explored qualitatively to determine their effectiveness. These new approaches lead to the development of even more active low-temperature catalysts for the hydrogen shift. The details of the various preparation techniques and the materials utilized are not included in this report, as this information is classified "Confidential".

Cocurrent with this effort, studies were performed to determine the effect of catalyst activation temperature, particle size, chamber diameter, and surface area on the conversion activity. Adsorption studies were also conducted to determine the physical and chemisorptive capacity of the advanced catalysts. A mathematical model based on a separation factor concept was developed to acquire a better understanding of the reaction kinetics involved in the low temperature ortho-parahydrogen conversion. An experimental apparatus for measuring the magnetic susceptibility was set up and calibrated and the techniques for analyzing experimental magnetic data were established.

III. THEORETICAL AND EXPERIMENTAL STUDIES

A. Activity Data on Improved Catalysts

The conversion activity of a series of improved catalysts prepared in our laboratory was determined at a pressure of 100 psig and a temperature of -320° F. Conversion data were obtained by measuring the parahydrogen concentration of a normal hydrogen (25% para) feed stream after passage through the catalyst chamber at various flow rates. Experimental data on the hydrous ferric oxide gel standard and on two of the most improved catalysts are presented in Table 1. These data are shown in plotted form in Figure 1 to illustrate how the relative conversion effectiveness was determined. The plot shows the percent parahydrogen in the effluent versus the flow rate of hydrogen expressed as grams of hydrogen per minute per gram of catalyst. The ratio of flow rates at a given effluent composition indicates the ratio of conversion activities. For example, from the table, the iron gel (20-5) showed 46.5% parahydrogen in the effluent at 0.199 grams H_2 per minute per gram of catalyst while the improved catalyst (10-2) showed a 46.3% parahydrogen composition at 1.61 grams H_2 per minute per gram of catalyst. The ratio of flow rates indicates that 10-2 can effect essentially the same degree of conversion at a flow rate eight times that at which the iron gel (20-5) can effect this degree of conversion. Since the fraction converted is the same in both cases, the quantity of hydrogen converted per unit time per unit mass of catalyst is a factor of eight higher with the improved catalyst than with the iron gel. Expressed another way, one pound of this improved catalyst properly activated will perform the same amount of conversion as eight pounds of the iron oxide gel under the same flow conditions.

Table 2 presents the conversion activity (relative to the iron gel reference) for a series of improved catalysts developed in our laboratory. Experimental data from the ortho-parahydrogen conversion reaction were used to determine these relative activities as described above for catalyst 10-2. In most cases, the surface area as determined by B.E.T. nitrogen adsorption measurements is also included. A direct correlation between activity and surface area is not illustrated but the trend that the higher area materials are generally the more active catalysts is apparent. This was shown by Weitzel, et al (1) in their work on hydrous ferric oxide gel catalysts. However, the type of promoter or paramagnetic material used in the catalyst will influence the relationship between surface area and activity. Further, the distribution of the promoter or active sites on the

TABLE 1

ORTHO-PARAHYDROGEN CONVERSION DATA*

Catalyst Number	Sample Weight (Gms)	Flow Rate (SCFM) at 70° C	Gms H_2/Min / Gm Cat	Concentration Feed (% Para-H_2)	Concentration Effluent (% Para-H_2)	Lbs. Cat. / Lb H_2/Sec	% Equilibrium
20-5 (70-80 mesh)	0.5812 1/8" I.D. chamber	0.0493	0.199	25.8	46.5	301	81.6
		0.0775	0.313	25.9	42.5	192	67.0
		0.1082	0.435	26.1	39.6	138	55.2
		0.1605	0.645	26.3	36.3	93	41.0
		0.1956	0.789	26.3	34.6	76	34.0
10-2 (70-80 mesh)	0.3978 1/8" I.D. chamber	0.0643	0.378	25.8	50.7	159	100.0
		0.1085	0.640	26.1	50.2	94	97.9
		0.1529	0.900	26.3	49.3	67	94.2
		0.1936	1.14	26.3	48.3	53	90.2
		0.2366	1.39	26.3	47.3	43	86.1
		0.2730	1.61	26.3	46.3	37	82.0
1049-100 (50-80 mesh)	0.2932 1/8" I.D. chamber	0.0499	0.398	25.5	50.7	150	100.0
		0,0962	0.768	25.3	50.0	78.1	97.3
		0.1523	1.215	25.3	48.6	49.4	91.8
		0.2001	1.600	25.3	47.1	37.5	85.8
		0.2541	2.030	25.3	45.6	29.5	79.9

*Conversion at 100 psig and -320° F.

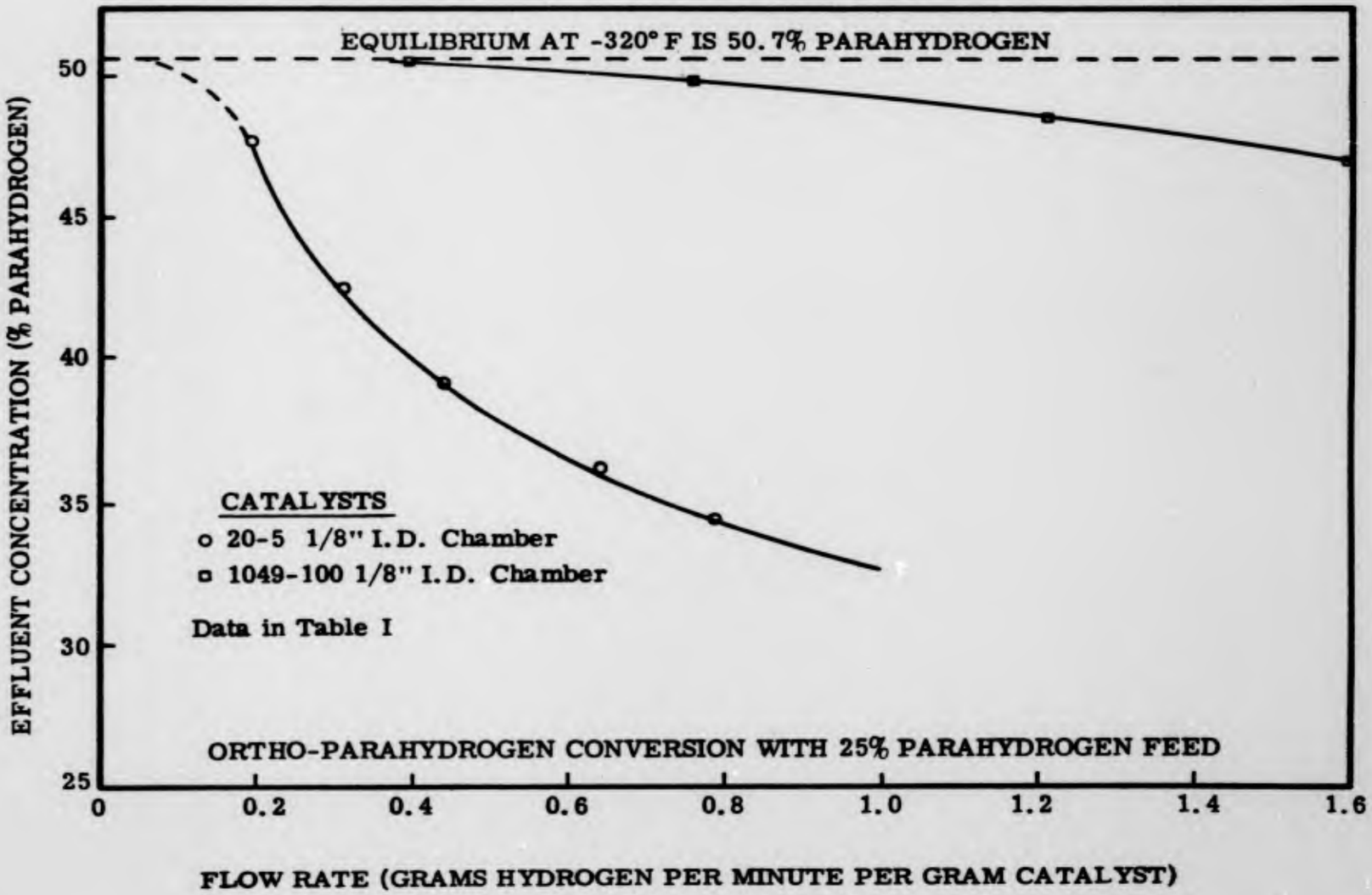

Figure 1 Catalyst Activities

TABLE 2

CONVERSION ACTIVITIES FOR IMPROVED CATALYSTS

Catalyst Identification Number	Particle Size (Mesh Size)	Surface Area (M^2/gm)	Conversion Activity (Relative to 20-5)
8	70-80	551	4.25
10-2	70-80	517	8.00
10-4	70-80	---	6.81
12-2	70-80	---	7.20
13-2	70-80	515	5.77
18-2	70-80	318	3.80
47	70-80	---	5.80
52	70-80	479	7.72
52-1	70-80	542	8.76
88	70-80	277	1.65
94-1	70-80	406	0.95
94-2	70-80	432	1.68
94-3	70-80	422	1.06
100	70-80	249	1.24
101	70-80	245	1.53
1049-100	50-80	---	9.70

surface and the availability of these sites provide variations in the correlation. Although high surface area materials are necessary to provide high activity catalysts, such characteristics as site concentration, site distribution and pore size are equally important.

Table 2 shows that several catalysts significantly more active than the iron gel reference have been developed and tested. The most active catalyst shown in the table exhibits an activity almost ten times greater than the standard iron gel when compared on a weight basis. The surface area of this material (1049-100) was not measured but is similar to sample (52-1) which has an area of 542 square meters per gram and a relative activity of 8.76.

The data presented in Table 3 shows para-orthohydrogen conversion data on both the iron gel standard (20-5) and the improved catalyst (10-2). These data were obtained by measuring the parahydrogen concentration of an essentially 99.8% parahydrogen feed stream after passage through the catalyst chamber at -320° F and 100 psig at various flow rates. These data are shown in plotted form in Figure 2 which illustrates that for the para to orthohydrogen conversion, catalyst (10-2) is again several times more effective than the iron oxide gel standard (20-5). Actual comparison shows that the relative activity is only six to seven times the iron gel for the para to ortho conversion while the relative activity is eight times for the reverse reaction. The conversion interval (99.8% para to 50.7% para at equilibrium) and thus the quantity of hydrogen converted is considerable with this improved catalyst. Therefore, the quantity of refrigeration developed in the catalyst bed by this endothermic para to orthohydrogen conversion tends to lower the bed temperature below that of the liquid nitrogen bath. Since the temperature of the catalyst determines the equilibrium parahydrogen concentration toward which the conversion proceeds, the conversion rate decreases as the conversion interval decreases. This effect is substantiated by data in Table 3 for para-orthohydrogen conversion with catalyst (10-2) in an 1/8" I.D. catalyst chamber and by Figure 2 where these data are plotted. With the 1/8" I.D. chamber, the equilibrium parahydrogen concentration for -320° F could not be established even at the lowest flow rates. This implies that heat transfer restrictions in this larger diameter bed permitted the establishment of a significant temperature gradient across the bed.

The data from Table 1 pertaining to the reference catalyst (20-5) and the improved catalyst (1049-100) for the ortho to parahydrogen conversion are presented in Figure 3 in a slightly different form. In Table I, columns seven and eight show the inverted flow rate expressed in pounds of catalyst per pound of hydrogen flow per second and the percent of equilibrium that

TABLE 3

PARA-ORTHOHYDROGEN CONVERSION DATA*

Catalyst Number	Sample Weight (Gms)	Flow Rate (SCFM) at 70° C	Gms H_2/Min		Concentration	
			Gm Cat		Feed (% Para - H_2)	Effluent (% Para - H_2)
20-5 (70-80 mesh)	0.6045 1/16" I.D. chamber	0.0253	0.0986		99.3	51.2
		0.0415	0.160		99.5	53.8
		0.0736	0.285		99.5	61.2
		0.0796	0.308		99.2	62.0
		0.136	0.511		99.3	69.7
		0.162	0.625		99.3	75.5
		0.204	0.796		99.3	78.3
		0.230	0.896		99.3	80.5
10-2 (70-80 mesh)	0.2940 1/16" I.D. Chamber	0.0326	0.260		99.5	50.7
		0.0623	0.495		99.5	51.3
		0.0920	0.732		99.5	52.7
		0.121	0.963		99.3	54.7
		0.152	1.21		99.5	57.2
		0.185	1.48		99.3	59.7
		0.218	1.74		99.0	62.0
10-2 (70-80 mesh)	0.4236 1/8" I.D. chamber	0.0041	0.0226		99.5	51.5
		0.0678	0.375		99.5	52.5
		0.0916	0.505		99.5	53.2
		0.120	0.663		99.5	54.3
		0.148	0.820		99.5	55.5
		0.182	1.01		99.3	57.0
		0.214	1.185		99.4	58.2
		0.242	1.33		99.0	59.3
		0.265	1.46		99.2	60.2

*Conversion at 100 psig and -320° F

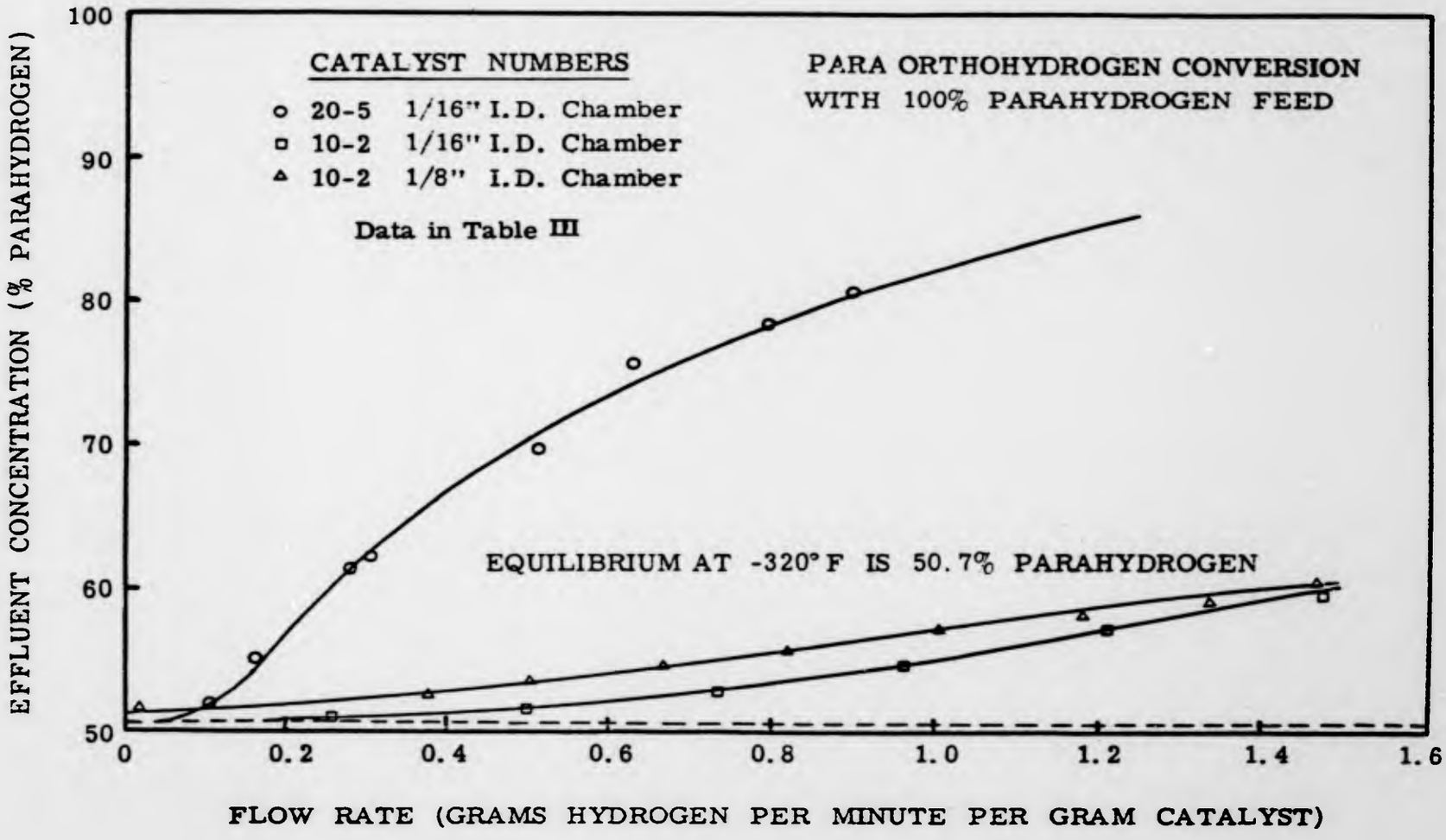

Figure 2 Catalyst Activities

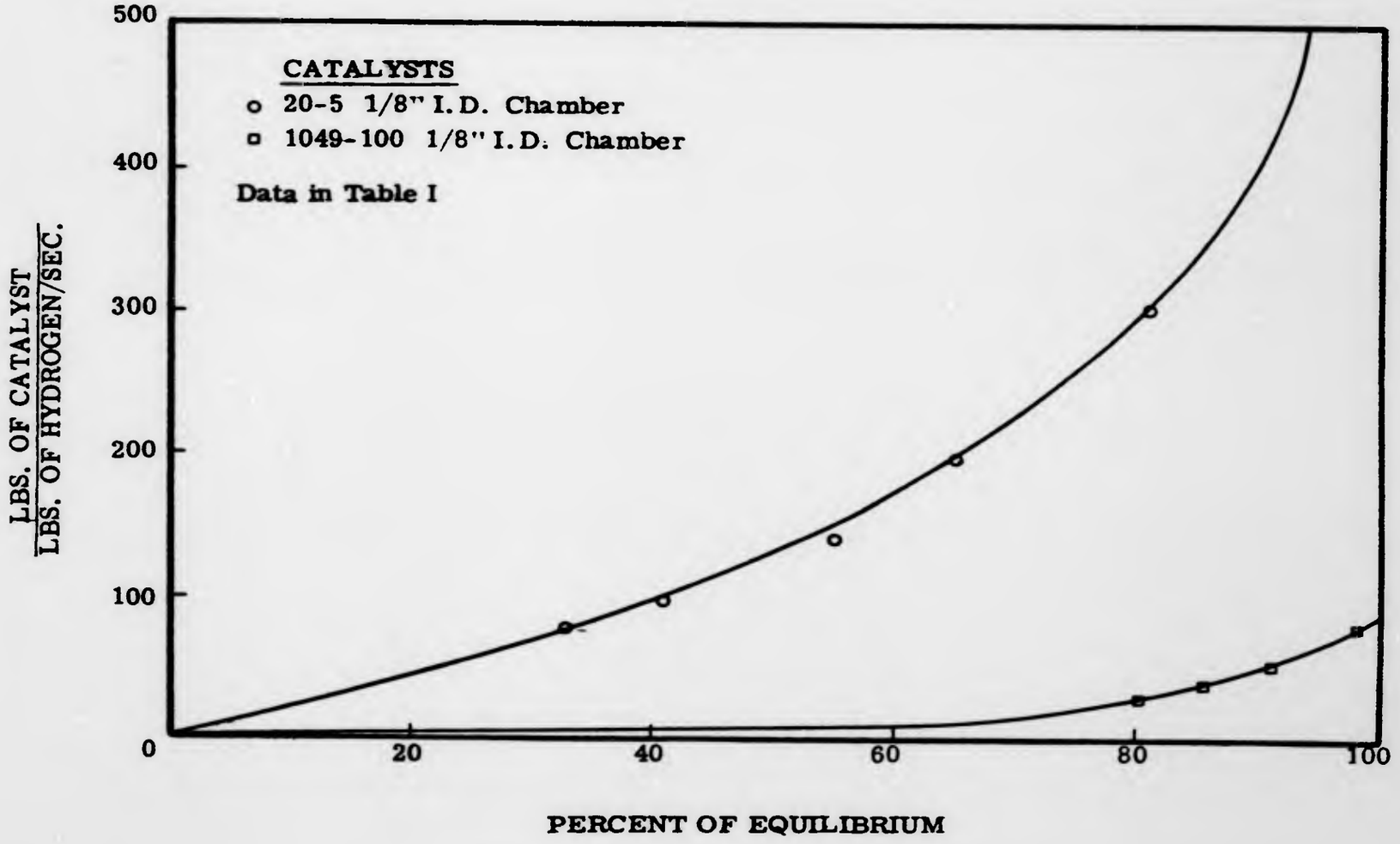

Figure 3 Weight of Catalyst Needed for Various Amounts of Conversion

is achieved for the various flow rates. The percent of equilibrium for ortho to parahydrogen conversion is defined as

$$\% \text{ Equilibrium} = \frac{C_i - C_o}{C_i - C_e} \times 100$$

where C_i is the mol fraction of orthohydrogen in the feed, C_o is the mole fraction of orthohydrogen in the effluent, and C_e is the mol fraction of orthohydrogen at equilibrium for the temperature of conversion. In Figure 3, the pounds of catalyst per pound of hydrogen flowing per second is plotted as a function of the percent of equilibrium achieved. The engineering advantages of the improved catalyst (1049-100) compared to the reference catalyst (20-5) are evident. In order to achieve 80% conversion with the hydrous ferric gel (20-5), about 290 pounds of catalyst per pound of hydrogen per second are required and with the improved catalyst (1049-100) only 29.5 pounds of catalyst per pound of hydrogen per second are necessary. A relative activity of 9.67 for sample (1049-100) is determined from the ratio of these quantitites. Alternatively, for a constant hydrogen flow rate, the weight of 20-5 to effect 40% conversion and the weight of catalyst (1049-100) to achieve almost complete conversion are the same.

B. Effect of Catalyst Activation Temperature on Conversion Activity

All catalysts prepared in the laboratory were activated before their conversion activity was experimentally determined. The catalysts reported in Tables I, II, and III were activated by passing dry, high purity hydrogen through the filled catalyst chamber for one hour while the chamber was immersed in an activation bath. The activation equipment which was utilized was relatively simple but quite effective for use with commercial catalysts exhibiting low conversion activities. This activation procedure was satisfactory for a qualitative appraisal of the effect of modifications of the starting materials and the preparation techniques on the catalyst conversion activity. The advanced catalysts which Air Products has been developing, however, are more sensitive to activation conditions than commercial catalysts. It was found that the activation technique which was used earlier in the catalyst development program was inadequate to permit reproducible high-temperature activations of the advanced catalysts. A new, high temperature activation apparatus, therefore, was designed and fabricated.

After the new activation apparatus was placed in operation, tests were begun to determine the optimum activation temperatures of several of the advanced catalysts. Several catalysts showed a significantly greater weight loss during

activation than previously experienced. The unsupported, hydrous ferric oxide gel catalyst (20-5) and advanced catalyst (1049-100), for example, showed additional weight losses of 6% and 15%, respectively when activated at their optimum activation temperatures. This means that the activities of both catalysts are actually higher than previously reported. The activity of advanced catalyst (1049-100) was previously reported as 9.67 relative to the standard iron gel standard (20-5). Through correction for this additional weight loss during activation of 9%, an activity of 10.5 times the iron gel standard was calculated for advanced catalyst (1049-100).

C. Effect of Catalyst Particle Size on Conversion Activity

A study of the effect of catalyst particle size on the conversion activity for one of the improved catalysts was performed. The catalyst was separated into various mesh size ranges by sieving. A U.S. Standard Sieve Series was used to accomplish this sizing. Samples of each size were packed in 1/4" I.D. x 1" long conversion chambers, activated by purging with high-purity, dry nitrogen at 150°C for two hours, and the conversion activity determined at -320°F and 100 psig. The results are tabulated below for catalyst 1049-51.

Mesh Size Range	Particle Size Range (microns)	Activity Relative to Iron Gel (70-80 mesh)
25-30	710 to 590	3.25) +10%
30-50	590 to 297	3.58) +15%
50-70	297 to 210	4.11) 0
70-80	210 to 177	4.08

These data indicate that the activity increases as the particle size decreases and this effect is attributed to internal or pore diffusion limitations in the catalyst. By reducing the particle size, the average pore length is reduced and the diffusion characteristics are improved until a point is reached beyond which no further improvement is observed. This particle size is considered to be that which exhibits no limitation to conversion activity as a result of diffusional restrictions. In effect, the total surface is available for conversion, whereas in larger particles, the interior surface cannot function efficiently because of mass transfer limitations.

D. Effect of Chamber Diameter on Catalyst Activity

The effect of chamber diameter on the apparent conversion activity was studied by measuring the conversion by an improved catalyst in various diameter chambers. All other parameters were held constant. Conversion data were obtained for the ortho-para shift at 100 psig and -320° F using three different inside diameter chambers, namely 1/4" I. D., 1/8" I. D., and 1/16" I. D. These data are presented in Table IV and illustrated in Figure 4 where the effluent parahydrogen concentration is plotted against the mass flow rate of hydrogen per unit mass of catalyst for the three different chamber diameters. With the 1/4" I. D. chamber, equilibrium hydrogen corresponding to the bath temperature could not be achieved even at the lowest flow rates because of the warming effect of the conversion on the catalyst bed. With the 1/8" I. D. chamber, the effect is less pronounced, and with the 1/16" I. D. chamber, equilibrium hydrogen is obtained at low flow rates indicating that the bed temperature is essentially that of the cryogenic bath. The data for the iron gel catalyst was included for comparison.

In Figure 5, a plot of the conversion rate versus the log-mean driving force is shown to illustrate the effect of chamber diameter. The deviation of the intercept from the origin is interpreted as an indication of the magnitude of the temperature interval between the catalyst bed and the cryogenic bath. Since C_e - the equilibrium composition - is defined by the bed temperature, any difference between bed and bath temperatures will be reflected in the log-mean driving force when C_e is chosen as a function of the bath temperature. The heat transfer requirements within the catalyst bed become more severe as the catalyst activities increase, since the increased conversion is accompanied by increased liberation or absorption of heat.

E. Effect of Surface Area on Conversion Activity

A special technique for increasing the surface area, and therefore the activity of a catalyst, has been qualitatively examined. The effects of this special technique are illustrated below, where the surface area and the activity, relative to the standard iron gel (sample 20-5) are presented for both specially treated and untreated samples for a given activation temperature. The special samples are designated as (-2) while the control samples are marked (-1).

TABLE 4

ORTHO-PARAHYDROGEN CONVERSION DATA*

Catalyst Number	Catalyst Weight (Gms)	Flow Rate (SCFM) at 70°F	Gms H_2/Min / Gm Cat.	Feed Concentration (% Ortho-H_2)	Effluent Concentration (% Ortho-H_2)	Fraction Converted $C_i - C_o$	Gms Converted/Min / Gm Cat.	$\frac{C_i - C_o}{\ln \frac{C_i - C_e}{C_o - C_e}}$
20-5	0.5812	0.0493	0.199	74.2	53.5	0.207	0.0412	0.122
(70-80 mesh)	1/8" I.D.	0.0775	0.313	74.1	57.5	0.166	0.0520	0.151
Activation at	x 2-1/2"	0.1082	0.435	73.9	60.4	0.135	0.0587	0.170
100°C with H_2	chamber	0.1605	0.645	73.7	63.7	0.100	0.0645	0.189
		0.1956	0.789	73.7	65.4	0.083	0.0655	0.198
1014-52-2	0.3494	0.0463	0.309	74.7	51.1	0.236	0.07292	0.0759
(70-80 mesh)	1/4" I.D.	0.1050	0.704	74.1	52.6	0.215	0.1514	0.0965
Activation at	x 1"	0.1726	1.155	73.8	53.8	0.200	0.2310	0.1090
300°C with N_2	chamber	0.2376	1.590	73.7	55.0	0.187	0.2973	0.1202
		0.2891	1.936	73.7	55.9	0.178	0.3446	0.1280
1014-52-2	0.3682	0.0424	0.269	74.7	49.6	0.251	0.0675	0.0565
(70-80 mesh)	1/8" I.D.	0.0989	0.628	74.1	50.2	0.239	0.1500	0.0499
Activation at	x 8"	0.1739	1.105	73.8	51.9	0.219	0.2420	0.0867
300°C with N_2	chamber	0.2303	1.465	73.7	53.5	0.202	0.2959	0.1056
		0.2820	1.798	73.7	54.7	0.190	0.3416	0.1175
1014-52-2	0.3129	0.0469	0.351	74.6	49.3	0.253	0.0888	.....
(70-80 mesh)	1/16" I.D.	0.0803	0.600	74.3	49.4	0.249	0.149	0.0451
Activation at	x 12"	0.1052	0.788	74.1	50.0	0.241	0.190	0.0676
300°C with N_2	chamber	0.1321	0.988	74.0	50.3	0.237	0.234	0.0739
		0.1692	1.265	73.8	51.5	0.223	0.282	0.0926
		0.2001	1.495	73.8	52.5	0.213	0.318	0.105
		0.2263	1.692	73.8	53.4	0.204	0.345	0.114
		0.2763	2.065	73.8	55.2	0.186	0.384	0.131
		0.3201	2.410	73.8	56.5	0.173	0.417	0.156

*Conversion at 100 psig and -320°F.

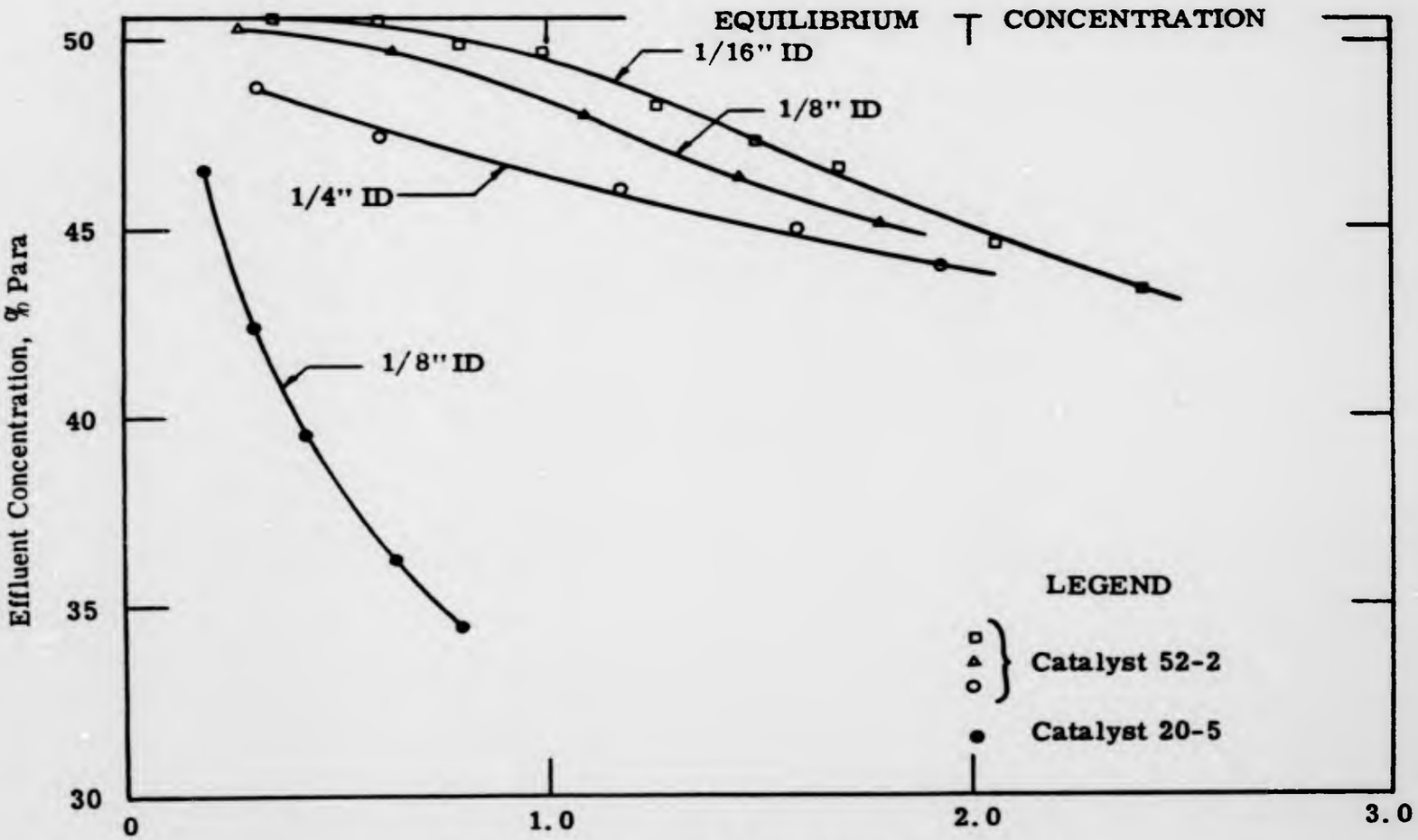

Figure 4 . Ortho-Para Conversion at 100 psig and -320° F with 25% Para Feed. Concentration Vs. Flow Rate

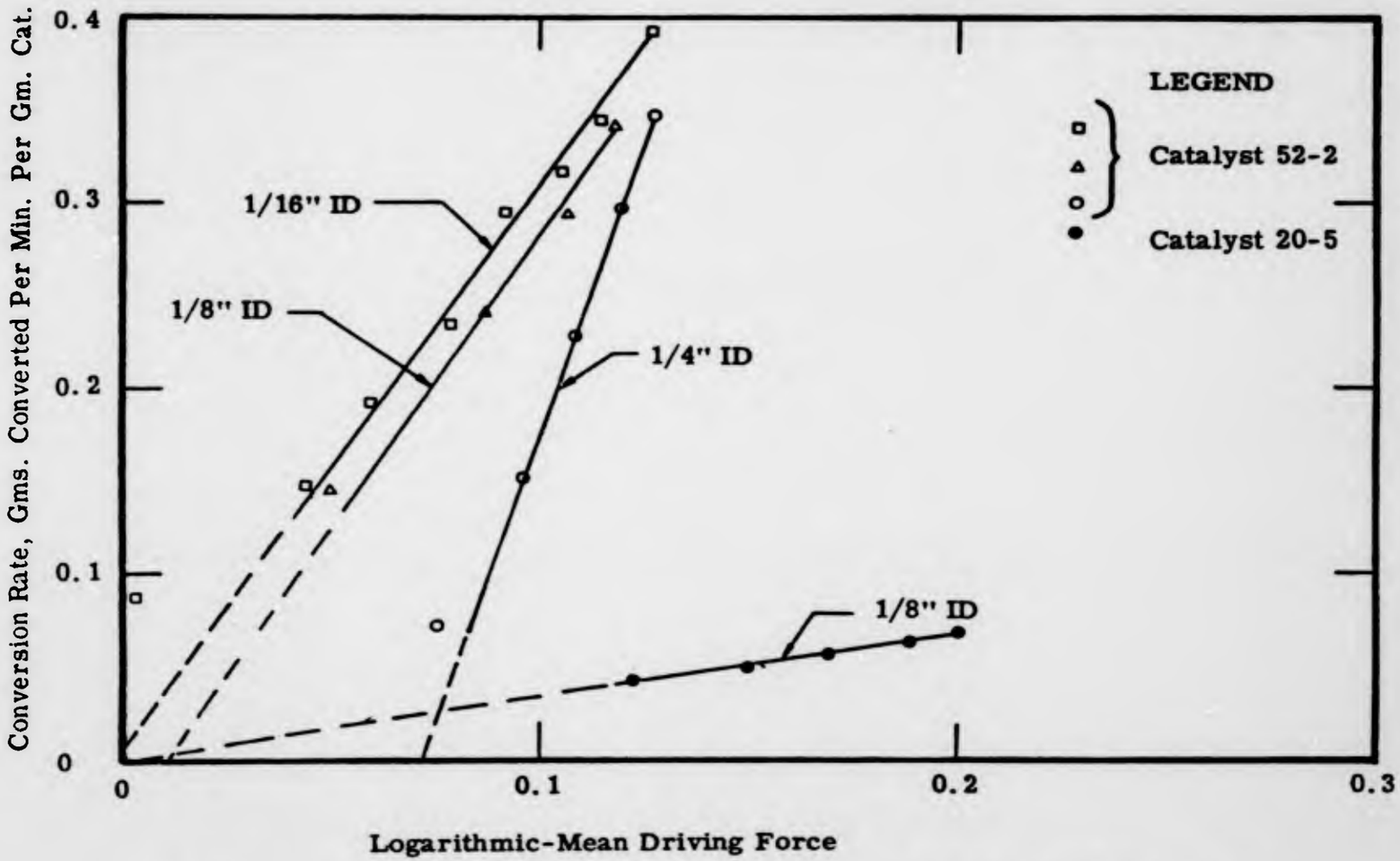

Figure 5 . Ortho-Para Conversion at 100 Psig and -320° F for 25% Para Feed.

Conversion Rate Vs. Logarithmic-Mean Driving Force

Catalyst Sample No.	Surface Area M^2/Gm	Activation Temp. °C	Relative Activity	% Change in Activity
52-1	479	145	4.60	
52-2	542	145	5.73	+24.6
19-A-1	321	150	1.90	
19-A-2	273	150	1.56	-17.9
26-1	256	130	4.59	
26-2	239	130	5.13	+11.8
26-1	256	155	5.60	
26-2	239	155	6.53	+16.6
28-1	309	250	4.44	
28-2	376	250	5.27	+18.7
30-1	555	150	2.19	
30-2	---	150	4.26	+94.5

This tabulation represents four samples of supported catalysts with different concentrations of promoter and one unsupported catalyst. The catalyst systems represented by numbers 52 and 28 show both an increase in surface area and an increase in activity as a result of this special treatment. Samples of number 26 exhibit an increase in activity but a paradoxical decrease in surface area. In the case of 19A which was the unsupported sample, the treatment resulted in a decrease in both surface area and activity. Number 30 exhibited a very significant increase in activity as a result of the special technique but the surface area of the treated sample is not yet available for comparison with the untreated sample.

Although the catalyst data resulting from special treatment does not show a clear-cut correlation between surface area and activity, only the unsupported catalyst (19-A) experienced a decrease in both. The four supported catalysts showed definite increases in activity after treatment, although the surface area did not reflect this gain in every case. It is anticipated that further examination of this procedure will broaden our understanding of this effect and ultimately provide additional improvements in catalyst activity.

F. Adsorption Studies

General

The purpose of the adsorption studies was to gain knowledge concerning the catalytic ortho-parahydrogen conversion mechanism. It was felt that a relationship might be established between physical adsorptive capacity and catalyst conversion activity, and between chemisorption capacity and catalyst conversion activity. Physical and chemisorption capacities are both related to the surface area of the solid catalyst sample but in different ways. Physical adsorption occurs on the surface of solids because valence or other attractive forces of the atoms or molecules in the outmost layer of the solid catalyst are not so fully utilized as in the interior of the solid. The extent of physical adsorption depends upon the specific nature of the catalyst and the molecules being adsorbed, temperature, and pressure. The forces causing physical adsorption are similar to those causing the condensation of a gas to liquid. The heat evolved during adsorption is small, the process is reversible, and the adsorbed molecules of gas may be several layers thick. Physical adsorption might be thought of as a measure of the surface area of the adsorbent. Quantitatively, chemisorption is generally of a smaller magnitude than physical adsorption and is not as strongly pressure dependent. In chemisorption a surface compound is formed and the heat evolved may be significant. The chemisorption process is irreversible and only a single chemisorbed layer may be formed. Chemisorption might be thought of as a measure of the number of chemically active sites on the surface of the adsorbent.

Experimental Apparatus

The experimental apparatus used for the adsorption studies is shown in Figure 6. The apparatus consisted of a catalyst test section and a measurement section. The catalyst test section consisted of a glass dewar into which was placed a stainless steel cylinder having a volume of about 75 ml. This cylinder was filled with a weighed catalyst sample. A sketch of this stainless steel catalyst chamber is shown in Figure 7. The two coiled heat exchangers on either side of the catalyst chamber were used for activating the catalyst sample prior to the performance of an adsorption test. A cover was placed on top of the dewar to prevent atmospheric contaminants from diffusing into the cryogenic fluid with which the dewar was filled during the tests. Quick connects with double-end shut-off valves were provided to facilitate installation of the catalyst chamber into the test section and to eliminate the possibility of contaminating the activated catalyst

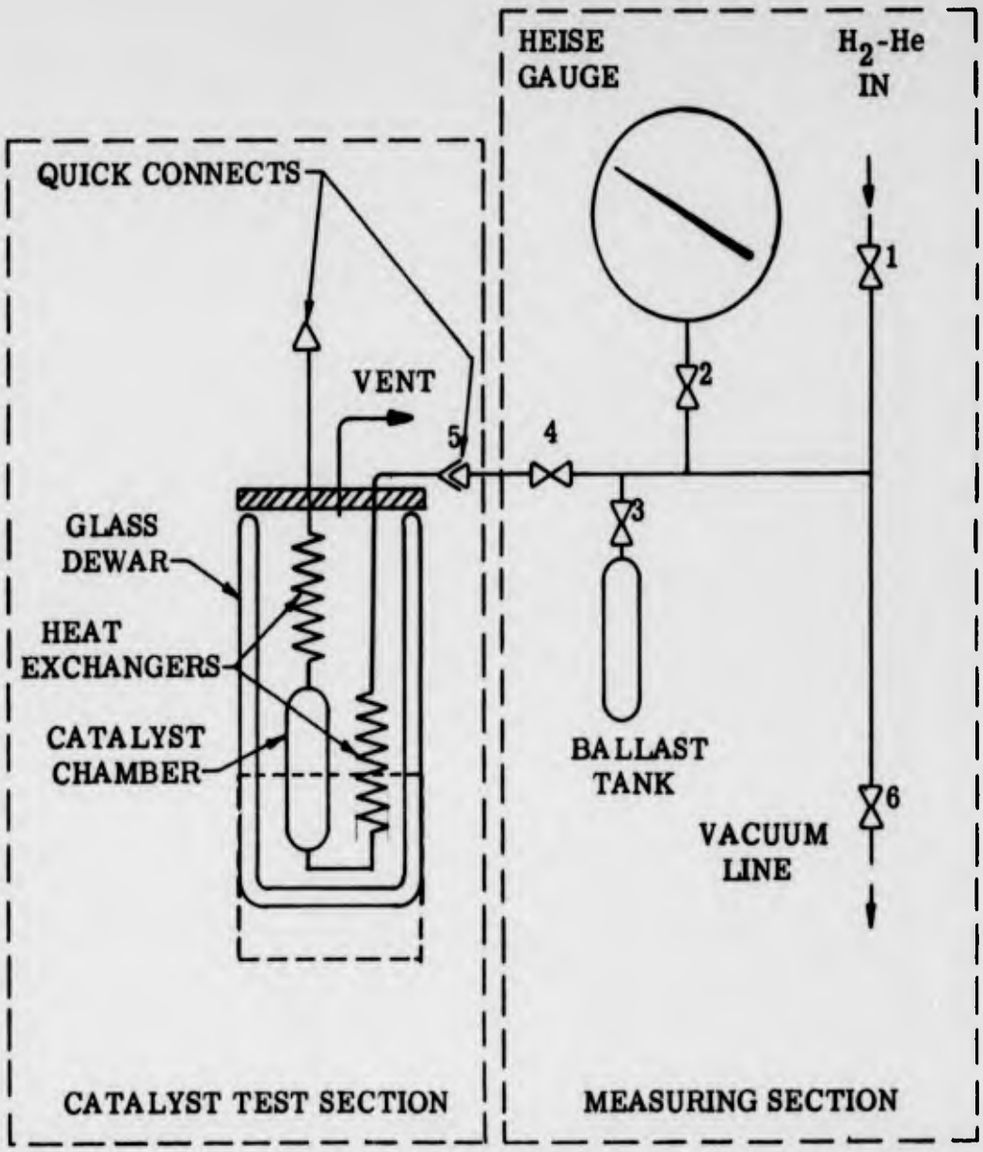

Figure 6 Experimental Apparatus for Adsorption Studies

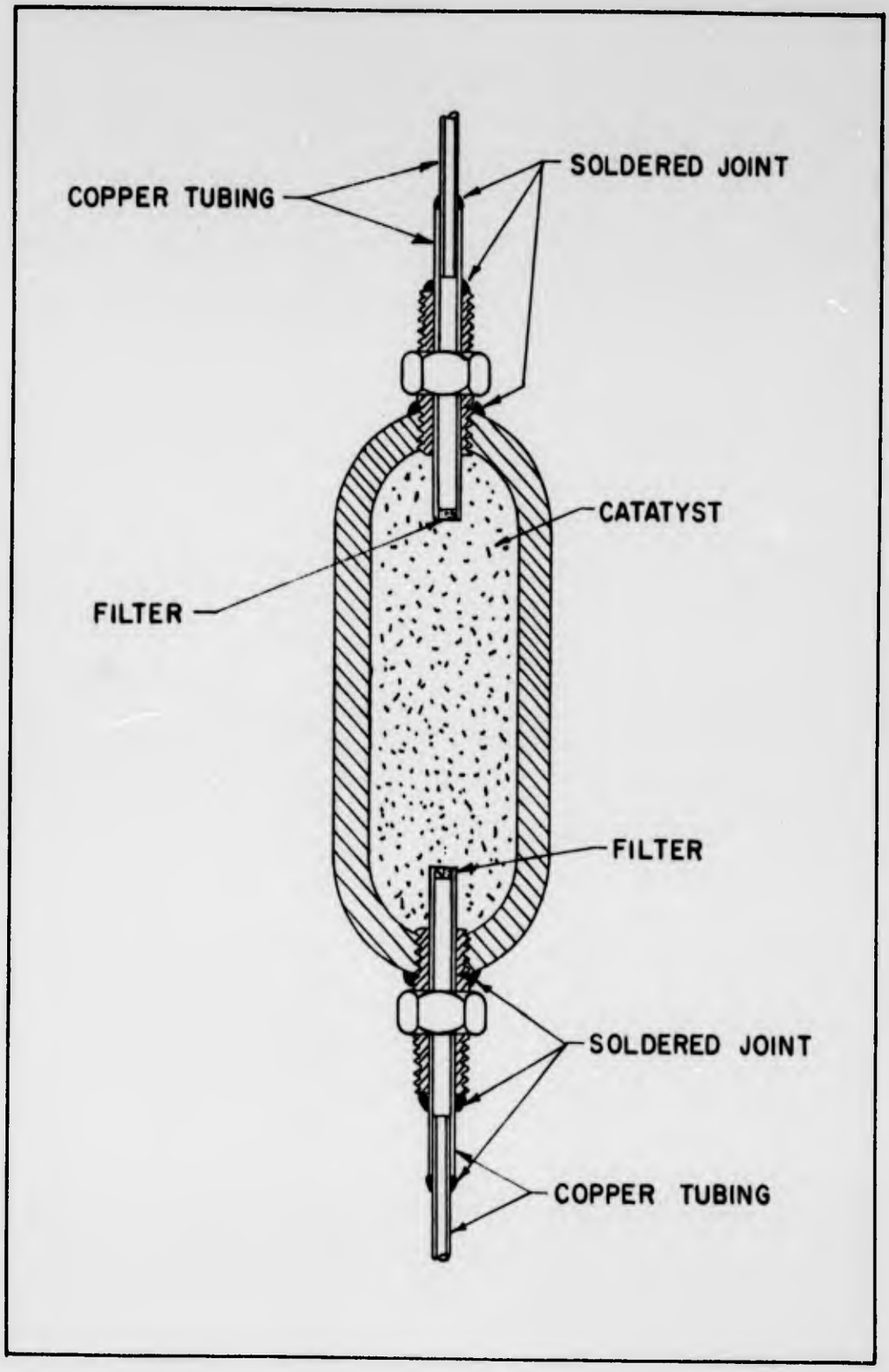

Figure 7 Construction of the Catalyst Chamber

sample with atmospheric air. The measuring section consisted of a sensitive, high-pressure, Heise gauge and a stainless steel ballast tank. A mechanical vacuum pump was connected to this section at valve 6.

The apparatus was assembled and leak checked by pressurizing it with helium. Both sections of the apparatus were volume calibrated in the manner described below.

The volume of the ballast tank was determined by filling it with demineralized water and noting the empty and filled masses. The mass of water required to fill the ballast tank was divided by the density of the water to obtain the volume of the ballast tank which was found to be 75.15 ml. The catalyst test section was disconnected from the measuring section at quick connect 5. Valves 1, 2, 3 and 6 were opened. The measuring section was evacuated to 10^{-4} Torr by means of the mechanical vacuum pump and valve 6 was closed. The section was then pressurized with helium by opening valve 1. Valve 1 was closed and the section allowed to attain an initial-charge, equilibrium pressure which was noted. Valve 3 was closed, valve 6 opened, and the section was evacuated to 10^{-4} Torr. Valve 6 was closed and valve 3 slowly opened. The final equilibrium pressure of the section was noted with valve 3 fully opened. The total volume of the measuring section was then calculated from the initial-charge and final equilibrium pressures and the volume of the ballast tank using the ideal gas law.

$$V = v_1 \left(1 + \frac{P_1}{P_2}\right)$$

where

V = total measuring section volume
P_1 = initial-charge equilibrium pressure
P_2 = final equilibrium pressure
v_1 = volume of ballast tank

The measuring section volume was calculated for several different initial-charge equilibrium pressures. The mean value of the calculated volumes was used as the volume of the measuring section.

The volume of the catalyst test section was determined in a similar manner with and without catalyst in the catalyst chamber.

Method of Operation

Each catalyst sample was activated before an adsorption test was begun. The measuring section was evacuated by opening valves 1, 2, 3 and 6 (See Figure 6). The catalyst chamber was cooled to room temperature and placed in the glass dewar filled with cryogenic fluid. The catalyst chamber was then connected to the pre-evacuated measuring section by quick connect 5 and valve 4 was opened slowly. When the pressure reached approximately 10^{-4} Torr, valves 4 and 6 were closed. The measuring section was charged with gaseous hydrogen through valve 1 and the initial-charge equilibrium pressure was noted. Valve 4 was slowly opened permitting hydrogen to enter the catalyst test section. The system reached equilibrium in about 15 minutes at which time the equilibrium pressure was noted. Valve 4 was closed and valve 1 was opened to recharge the measuring section to a pressure slightly higher than the initial-charge pressure. Valve 4 was slowly opened permitting hydrogen to enter the test section. When equilibrium was reached the equilibrium pressure was noted. This procedure was repeated several times until the equilibrium pressure reached 400 psig. Test temperatures of 63.16°K, 77°K, 87.8°K and 194.6°K respectively, were obtained by filling the glass dewar with liquid nitrogen under vacuum, liquid nitrogen at atmospheric pressure, liquid argon, and an acetone-dry-ice mixture.

Method of Calculation

The volume of gas adsorbed by the catalyst surface under equilibrium conditions was calculated from the equation developed below.

$$N_{ad} = \frac{P_o V_{aux}}{R T_{aux}} + (P_1 - P_1') \frac{V_{aux}}{R T_{aux}} + (P_2 - P_2') \frac{V_{aux}}{R T_{aux}} + \cdots$$

$$(P_{n-1} - P_{n-1}') \frac{V_{aux}}{R T_{aux}} + (P_n - P_n') \frac{V_{aux}}{R T_{aux}} - P_n' \left(\frac{V_{aux}}{R T_{aux}} + \frac{V_{cat}}{R T_{cat}} \right)$$

denoting differences $P_1 - P_1'$, $P_2 - P_2'$, ... $P_{n-1} - P'_{n-1}$, $P_n - P_n'$ by $\Delta P_1, \Delta P_2 \ldots . \Delta P_{n-1}, \Delta P_n$ respectively we have

$$N_{ad} = P_o + \sum_{n=1}^{n=n} \Delta P \quad \frac{V_{aux}}{R T_{aux}} - \frac{P_n'}{R} \left(\frac{V_{aux}}{T_{aux}} + \frac{V_{cat}}{T_{cat}} \right) \qquad (1)$$

where

V_{aux} = volume of the auxiliary system, ml
V_{cat} = volume of the catalyst system, ml
T_{aux} = temperature of the auxiliary system, °K
T_{cat} = temperature of the catalyst system, °K
N_{ad} = number of moles of gas adsorbed
R = gas constant, $\frac{\text{atms-ml}}{\text{gm moles-°K}}$
P_o, P_1, P_2, P_3, ... P_{n-1}, P_n = the first and subsequent charge pressures, atms
P_1', P_2', P_3', ... $P_n'-1$, P_n' = the first and subsequent equilibrium pressures, atms

Adsorption Tests

Two catalyst materials, a ferric oxide iron gel designated 20-5 and an advanced type designated 1049-100, were tested at 63.16°K, 77.0°K, 87.8°K, and 194.6°K. No appreciable chemisorption is expected at these temperatures. Data taken for each run included the mass of the catalyst sample, the measuring section temperature, the catalyst test section temperature, and a series of initial-charge and final equilibrium pressures. The raw data for a typical run are shown in Table 5. Equation 1 was used to calculate the number of moles of hydrogen adsorbed by the catalyst for each final equilibrium pressure. The test data is summarized in Tables 6 through 9. Figure 8, showing the volume of hydrogen adsorbed per gram of catalyst versus final equilibrium pressure with temperature as a parameter, was plotted from the data presented in Tables 6 through 9.

Chemisorption Tests

Chemisorption tests were run on catalysts 20-5 and 1049-100 at room temperature and 100°C, and on catalyst 20-5 at 150°C. This was the extent of the chemisorption tests because of the time limitation imposed by the contract. The maximum chemisorption observed was 3 ml per gram for catalyst 1049-100 at 100°C. The chemisorption data are not shown on Figure 8 because of the difficulty in plotting these relatively small values.

TABLE 5

A TYPICAL DATA RUN - RUN 1

Catalyst: 1049-100 Weight: 36.2966 gms.

Temperature of Auxiliary System	Temperature of Catalyst System	No.	Initial Pressure P, psia	Equilibrium Pressure P', psia
300°K	77°K Bath Coolant Liquid Nitrogen	0	295.50	14.50
		1	200.00	39.25
		2	199.75	67.00
		3	200.25	93.00
		4	200.00	115.25
		5	249.50	143.75
		6	300.00	178.50
		7	399.00	228.50
		8	495.50	290.00
		9	496.50	339.00

CALIBRATED VOLUMES:

Volume of Auxiliary System	119.1 ml.
Volume of Catalyst System	81.4 ml.
Volume of Ballast Tank	75.1 ml.

TABLE 6

ADSORPTION DATA FOR HYDROGEN AT 63.16°K

Catalyst: 20-5 Weight: 90.0899 gms.		Catalyst: 1049-100 Weight: 36.2966 gms.	
Equilibrium Pressure P', atms.	Volume Adsorbed Per Gm., Cat., ml.	Equilibrium Pressure P', atms.	Volume Adsorbed Per Gm., Cat., ml.
0.221	11.6	0.0	20.4
1.16	19.1	0.306	57.0
2.62	23.4	1.28	83.4
3.94	25.7	3.84	106
5.15	27.3	6.70	117
6.16	28.3	1.28	84.4
9.03	30.9	6.00	117
11.3	33.3	11.2	130
15.6	36.7	15.7	138
19.0	39.0	19.3	144
22.1	41.2	22.1	149
24.6	42.9		
26.6	43.5		
28.0	45.3		

TABLE 7

ADSORPTION DATA FOR HYDROGEN AT 77° K

Catalyst: 20-5 Weight: 90.0899 gms.			Catalyst: 1049-100 Weight: 36.2966 gms.	
Equilibrium Pressure P', atms.	Volume Adsorbed Per Gm:, Cat:, ml.		Equilibrium Pressure P', atms.	Volume Adsorbed Per Gm:, Cat:, ml.
0,408	6,53		*0	10,3
1,16	11,1		*0.034	20.2
2,08	14.0		*0.136	34.4
2,98	15,8		0.986	48.7
4,12	17,4		2.67	67.0
5.46	19.0		4.56	77.9
6.90	20.3		6.33	84.6
8.47	21.4		7.84	88.9
10.1	22.6		9.78	93.8
11,8	23,6		12.1	98.3
13,4	24.9		15.5	105.
15.0	26.0		19.7	110.
			23.1	114

* Experimental data for these points are not included in Table 5.

TABLE 8

ADSORPTION DATA FOR HYDROGEN AT 87.8°K

Catalyst: 20-5 Weight: 90.0899 gms.		Catalyst: 1049-100 Weight: 36.2966 gms.	
Equilibrium Pressure P', atms.	Volume Adsorbed Per Gm., Cat., ml.	Equilibrium Pressure P', atms.	Volume Adsorbed Per Gm., Cat., ml.
0.476	4.31	0.221	18.2
1.43	8.08	0.816	31.6
2.81	11.1	2.69	50.4
4.49	13.4	6.22	66.2
6.36	15.3	11.05	78.1
8.67	16.9	4.06	58.3
11.8	18.7	10.7	77.9
15.9	20.6	16.5	86.3
20.8	22.5	21.0	90.7
24.5	23.5	24.5	92.9
27.1	24.1	27.0	94.7
		28.8	96.1
		30.2	96.7

TABLE 9

ADSORPTION DATA FOR HYDROGEN AT 194.6°K

Catalyst: 20-5 Weight: 90.0899 gms.		Catalyst: 1049-100 Weight: 36.2966 gms.	
Equilibrium Pressure P', atms.	Volume Adsorbed Per Gm., Cat., ml.	Equilibrium Pressure P', atms.	Volume Adsorbed Per Gm., Cat., ml.
0.952	0.123	1.38	1.45
2.84	0.494	3.67	3.15
4.69	0.742	6.12	7.17
6.46	0.998	0.56	7.72
8.20	1.23	12.8	9.47
10.7	1.58	16.1	11.1
15.2	2.19	19.5	12.5
20.7	2.96	22.8	13.9
27.1	2.98	26.3	15.3
30.1	3.79	29.6	16.7

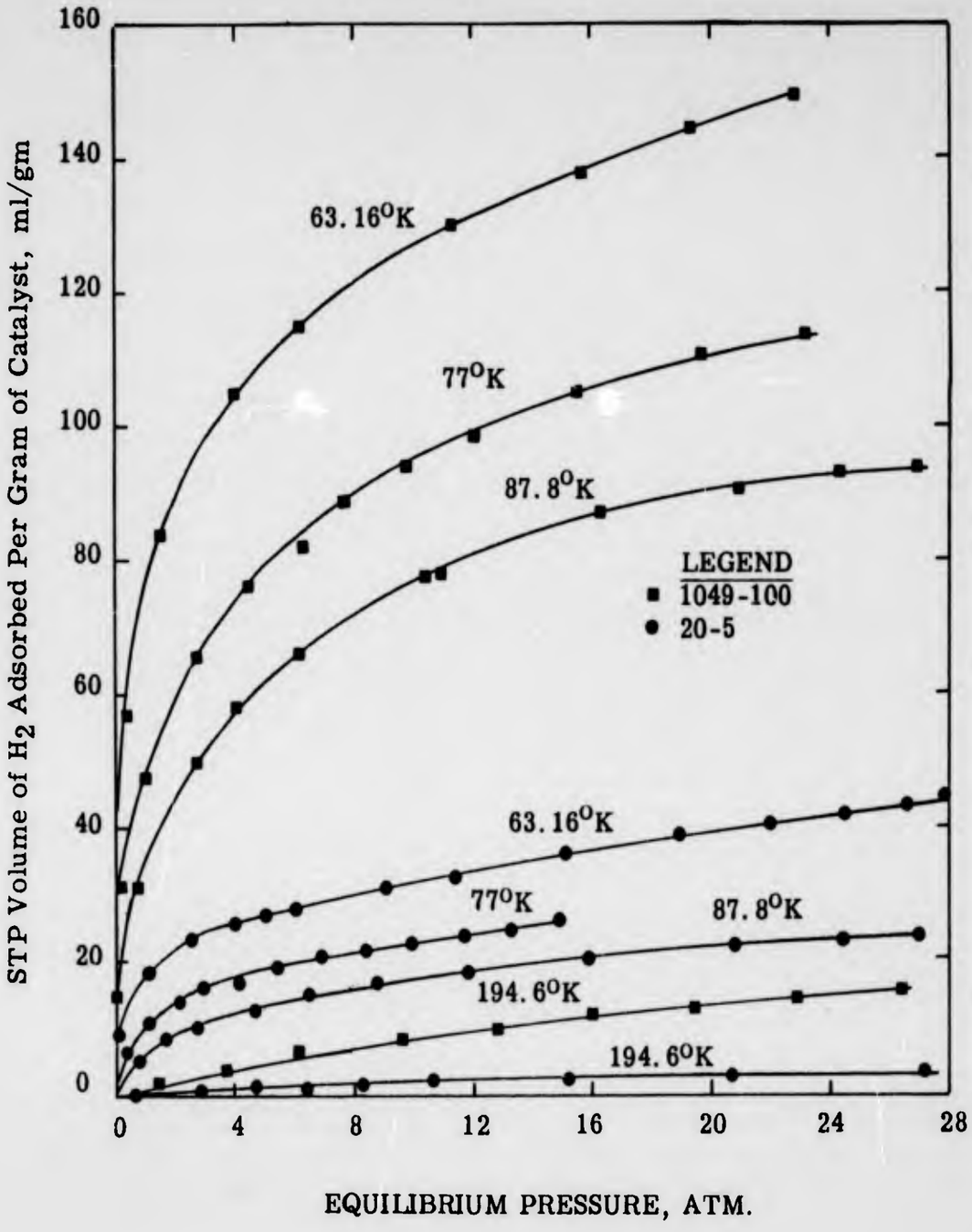

Figure 8: Hydrogen Adsorption Isotherms

G. Separation Factors of Advanced Catalysts

The development of a mathematical model was undertaken in an effort to acquire a better understanding of the reaction kinetics involved in the low temperature ortho-parahydrogen conversion in a packed catalyst bed. The model involves the preferential adsorption of orthohydrogen on the catalyst surface. This preferential adsorption phenomenon was first observed by Sandler[2]. The relative adsorbability of orthohydrogen and parahydrogen, referred to as the separation factor, was defined by Sandler as the ratio of concentrations of the two species in the adsorbed phase as compared to that in the gas phase. Later Cunningham and Johnston[3], utilizing the Sandler concept, developed a mathematical representation of the process of conversion of ortho to parahydrogen on a catalytic surface. The Cunningham-Johnston approach provides a technique of analyzing the experimental data for values of separation factor. It is expected that the separation factor is strongly a function of temperature and is essentially independent of the nature of the catalyst surface.

The Cunningham-Johnston equation when written in the form presented below provides the means of analyzing dynamic conversion data for the evaluation of separation factor. The derivation of this equation is given in Appendix I. The expression is:

$$\frac{1}{LMDF} = \frac{k_1 S V_R}{(1-C_e)\ 1 + (S-1)\ C_e} \cdot \frac{1}{V(C_i-C_o)} - \frac{S-1}{1 + (S-1)C_e}$$

The symbols used in the above equation are defined as follows:

LMDF = Logarithmic Mean Driving Force, $\dfrac{C_i-C_o}{\ln \dfrac{C_i-C_e}{C_o-C_e}}$

V_R = chamber volume, ft^3
k_1 = reaction rate constant, 1/min
V = gas velocity, ft^3/min
C_i = inlet concentration of ortho, mole fraction
C_o = outlet concentration of ortho, mole fraction
C_e = equilibrium concentration of ortho, mole fraction
S = separation factor

Thus when 1/LMDF is plotted versus $1/V(C_i-C_o)$, a straight line should result. The slope and intercept of the line will depend on the value of the separation factor, S. However, the separation factor could be evaluated from the knowledge of the intercept alone.

The above method of analysis was applied to the experimental data obtained on the catalysts developed in our laboratories. Initial analysis with low activity catalysts were encouraging and the results obtained thereby were consistent with published values. However, for highly active catalyst the results were not sufficiently accurate. The intercept of the plot 1/LMDF vs. $1/V(C_i-C_o)$ is sensitive, especially for high slope, to small variations in activity. For this reason the bed must be operated isothermally. With the highly active catalysts the internal bed temperature may be different from the temperature of the bath. Reducing the chamber diameter has helped somewhat to maintain isothermality. With more active catalysts the chamber size needed to maintain a uniform temperature in the bed becomes impractical. In spite of the experimental difficulties encountered during the application of this model it is believed that this model is a better representation of the process than the one which does not take into account the preferential adsorption.

In Table 10 are presented the values of separation factor calculated for three different catalysts. 20-5 and 65 are commercially available iron gel and iron oxide on alumina respectively. Sample 10-2 is one of the most active catalyst developed to date. The three different low temperatures, namely -297, -320 and 346° F were obtained by using liquid oxygen, liquid nitrogen and liquid nitrogen under vacuum baths, respectively. The increase in the value of the separation factor with decrease in temperature is in agreement with prediction.

TABLE 10

CALCULATED SEPARATION FACTORS

Catalyst	Activation Temperature, °C	Chamber Diameter, (I.D.)	Conversion Temperature, °F	Activity Relative to 20-5 @-320°F	Separation Factor
20-5	100	1/8"	-320	1.0	1.86
10-2	300	1/8"	-320	8.0	1.50
65	150	1/4"	-297	0.26	1.14
65	150	1/4"	-230	0.33	1.22
65	150	1/4"	-326	0.37	1.35

H. Magnetic Properties of Conversion Catalysts

General

Studies of the magnetic properties of catalysts were conducted as part of this laboratory's efforts, under Contract Nr. AF 33(616)-7506, to investigate the low-temperature para-ortho shift in hydrogen. The purpose of the studies was to generate fundamental information about the magnetic properties of the catalysts being developed. It was felt that this information would contribute to a sound understanding of the relationships between the catalyst preparation techniques and the observed conversion activities. In this report, the techniques for the analysis of experimental magnetic data will be discussed.

An effective catalyst for the hydrogen-shift reaction at cryogenic temperatures must have three primary characteristics. It must have a high physical adsorptive capacity for hydrogen, a high concentration of "active" or magnetic specie and a high paramagnetic moment of that specie. In 1933, Taylor and Diamond[4, 5] showed that paramagnetic substances are better low temperature conversion catalysts than are diamagnetic substances. Farkas and Sandler[6] and Turkevich and Selwood[7] showed that low-temperature, heterogeneous catalysis of the para-orthohydrogen conversion could be ascribed to the influence of the inhomogeneous magnetic field of the paramagnetic component of the catalyst upon the physically adsorbed hydrogen. Wigner[8] and Kalckar and Teller[9] developed theoretical treatments of the paramagnetic conversion. Their results are the prediction that the low temperature catalytic activity is proportional to the square of the magnetic moment of the paramagnetic molecule and to the inverse sixth power of the distance of closest approach of the hydrogen to the paramagnetic molecule. These predictions were substantiated by Farkas and Sachsse[10] who studied the effect of paramagnetic ions in solution and of dissolved oxygen on the conversion of hydrogen. Although Wigner's original theory was applicable for dilute homogeneous catalysis, Buyarnov[11] has demonstrated that the theory also applies for dilute heterogeneous catalysis.

Analysis of Experimental Magnetic Susceptibility Data

To measure the paramagnetic susceptibility of a material, the sample is placed in an inhomogeneous magnetic field and the force exerted on the sample by the field is measured. By the Faraday method, the size of the sample used is small with respect to variations in the gradient of the field. In this case, the force exerted on the sample is calculated by means of any one of the following relations:

$$\text{Force} = \chi m_o H \frac{\delta H}{\delta S} \quad (1)$$

$$= \sigma m_o \frac{\delta H}{\delta S} \quad (2)$$

$$= \kappa v H \frac{\delta H}{\delta S} \quad (3)$$

$$= \theta v \frac{\delta H}{\delta S} \quad (4)$$

where m_o is the mass of the sample, v is the volume of the sample, H is the strength of the magnetic field in which the sample is located, $\frac{\delta H}{\delta S}$ is the gradient of the field in the direction of the axis of symmetry of the field, χ is the magnetic susceptibility per unit mass, σ is the specific magnetization, or the magnetic moment per unit mass, κ is the magnetic susceptibility per unit volume, and θ is the intensity of magnetization, or the magnetic moment per unit volume. For measurements on solid samples, the utilization of equations 1 and 2, above, is considered to be the most convenient. χ is the desired quantity for the present studies and equation 1 will be utilized.

In this laboratory the sample will be suspended between the poles of an electro-magnet by a thread which is attached to the weighing pan of a sensitive analytical balance. Because the analytical balance indicates the apparent mass of the sample, equation 1 has been rearranged to the form:

$$\chi = \frac{980}{H \, \delta H / \delta S} \left(\frac{m - m_o}{m_o}\right) \quad (5)$$

where m is the apparent mass of the sample with the magnetic field turned on and m_o is the mass of the sample with no current in the electro-magnet. The fundamental units of χ are $(\text{length})^3/\text{mass}$. When all measurable quantities in equation 5 are expressed in cgs units, it is common practice to consider the dimension of χ as "cgs". χ_m, the molar susceptibility, or the susceptibility of Avogadro's number of paramagnetic atoms, can be calculated from the mass susceptibility derived above if the composition of the sample is known.

A generalized curve showing the variation of χ_m with temperature is presented below.

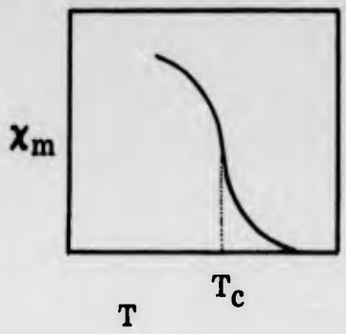

The temperature corresponding to the inflection point of the curve is called the Curie point. Above the Curie point, the susceptibility is independent of the strength of the magnetic field and is represented, in many cases[12] by the Curie-Weiss law derived theoretically by Weiss[13].

$$\chi_m = \frac{C}{T - \Delta} \qquad (6)$$

where C is the Curie-Weiss constant and Δ is the Weiss constant. In this temperature region, the material exhibits paramagnetic properties. Below the Curie point, the material is a ferromagnetic. The susceptibility does not vary with the inverse of the temperature and is dependent, in a complicated manner, upon the strength of the magnetic field. The Curie-Weiss constant must be evaluated as part of the calculation of the magnetic moment and the number of unpaired electrons per molecule. For this reason, all measurements will be made above the characteristic Curie temperature for the material being studied.

Occasionally, paramagnetic materials contain traces of ferromagnetic impurities. Since the susceptibilities of ferromagnetic materials may be orders of magnitude higher than paramagnetic susceptibilities, minute traces of ferromagnetic impurities can be readily detected. The effect of the impurity can be eliminated quite simply, however, by making measurements, for a given temperature, at two or more magnetic field strengths. The magnetic susceptibility can be plotted versus the reciprocal field and the trend can be extrapolated to infinite magnetic field, i.e., to $1/H = 0$. Extrapolation in this manner corresponds to saturation of the ferromagnetic impurity in an infinite magnetic field. At saturation, the ferromagnetic domains become completely oriented and the susceptibility is independent of the field strength. In other words, at saturation

a ferromagnetic material becomes paramagnetic. The saturated susceptibility is the sum of the paramagnetic contributions of both the sample and the impurity. As the impurity is generally present in trace amounts only, the extrapolated susceptibility is considered to represent the characteristics of the paramagnetic sample alone.

To continue the analysis of magnetic data, the inverse of the extrapolated molar susceptibilities are plotted versus temperature. The reciprocal of the slope of the resulting trend is numerically equal to the Curie-Weiss constant, C. From both the slope and the intercept of the line with the temperature axis, Δ/C, the value of the Weiss constant can be calculated. A representative plot is shown below. The above relationships can be verified analytically by solving Equation 6 for the reciprocal susceptibility as a function of temperature.

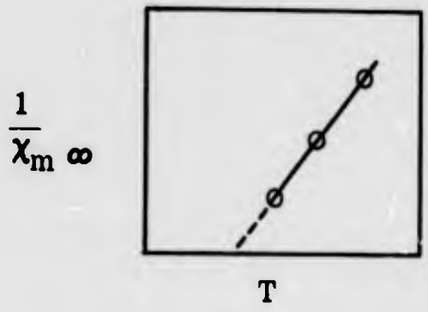

Analytically, the constants can be calculated by means of the expressions:

$$\Delta = \frac{\chi_{m\infty 1} T_1 - \chi_{m\infty 2} T_2}{\chi_{m\infty 1} - \chi_{m\infty 2}} \qquad (7)$$

and

$$C = (T_2 - T_1) \frac{\chi_{m\infty 1} \cdot \chi_{m\infty 1}}{\chi_{m\infty 1} - \chi_{m\infty 2}} \qquad (8)$$

where the subscripts 1 and 2 refer to properties at two different temperatures, as indicated in the above plot.

The effective Bohr magneton number, or the effective magnetic moment, may be computed by utilizing the relation[14]:

$$\mu_{eff} = \sqrt{\frac{3k\,\chi_{m\infty}(T-\Delta)}{N\beta^2}} = \sqrt{\frac{3kC}{N\beta^2}} = 2.839\sqrt{C} \qquad (9)$$

where k is the Boltzmann constant, N is Avogadro's number and β is 9.27×10^{-27} erg/gauss, the magnitude of the Bohr magneton.

For the transition group elements, the relationship between the effective magnetic monent, μ eff, and the number of unpaired electrons per paramagnetic atom, n, is approximately represented by the expression[15]:

$$\mu \text{ eff} = \sqrt{n(n+2)} \tag{10}$$

This formula has been rearranged to the form:

$$n = \sqrt{\mu^2_{\text{eff}} + 1} - 1 \tag{11}$$

The value of n, calculated by means of the above equations will be the desired result of the measurements of the magnetic susceptibility of catalyst samples.

IV. SUMMARY AND CONCLUSIONS

The existence of the ortho and para modifications of molecular hydrogen is a direct result of the orientation of the nuclear spins associated with the hydrogen atoms of the molecule. In molecular hydrogen, the nuclear spins of the individual atom are oriented either in the same direction (parallel) which corresponds to the ortho modification, or in the opposite direction (antiparallel) which corresponds to the para modification. These two orientations of nuclear spins are responsible for the difference in the magnetic and thermal properties of the ortho and para modifications of molecular hydrogen. An equilibrium, which is a function of temperature, exists between these two forms. Under equilibrium conditions, the para-hydrogen concentration varies from essentially 100% para at 20° K to approximately 25% para at 150° K. Since the para to orthohydrogen conversion is endothermic in this temperature range (339 calories per mole), certain additional low-temperature refrigeration is available from this conversion.

The investigation was concentrated on the area of low-temperature heterogeneous magnetic field of the paramagnetic component of the catalyst upon the physically adsorbed hydrogen. On this basis, an effective conversion catalyst should exhibit a high surface area or physical adsorptive capacity for hydrogen and a high density of paramagnetic sites on the surface.

An extensive catalyst development program has provided catalyst materials with increased effectiveness for the hydrogen conversion reaction through the optimization of such catalyst properties as physical adsorptive capacity or surface area, concentration of paramagnetic component and the magnetic moment of the paramagnetic component. A catalyst has been developed in our laboratory that exhibits an activity on a weight basis which 10.5 times that of the standard NBS-type hydrous ferric oxide gel. It is anticipated that the development of catalyst systems which make available higher percentages of the structural material as internal surface with uniform distribution of paramagnetic sites throughout this surface will provide significantly greater improvements in activity.

A study of the relationship between catalyst particle size (mesh size) and catalyst conversion activity for several different catalysts showed that the para-orthohydrogen conversion activity increased as the particle size decreased. This particle size effect is caused by the limited diffusion of the

flowing hydrogen into the interior regions or pores of the larger particles. This diffusion limits the complete utilization of the active surface of the catalyst. It is concluded that, with large particles, internal (pore) diffusion is a controlling mechanism of the over-all conversion process. With fine particles, the Thiele effectiveness factor approaches unity which indicates that pore diffusion is no longer limiting.

The study of the effect of chamber diameter on conversion activity suggested that non-isothermal conversion occurred in the catalyst chamber as a result of the limiting heat transfer between the bulk gas phase at the center of the packed bed and the inside chamber wall. In other words, the catalyst bed was not at the same temperature as the cryogenic liquid surrounding the chamber. This particular heat transfer process, as shown by calculations, was significantly more restricted than any of the other heat transfer mechanisms involved. The heat transfer requirements within the catalyst bed become more severe as the catalyst activities increase, since the increased conversion is accompanied by increased adsorption and liberation of heat. With advanced catalyst systems, essentially isothermal conversions were obtained with chamber diameters of 1/16" I.D.

No definite relationship between surface area and conversion activity could be established, however, the experimental data indicated that, in general, the catalysts with the higher surface areas exhibited the higher conversion activities. The surface area effect is considered the result of an increase in available sites which normally accompanies an increase in surface area. In addition, an increase in surface area provides an increased hydrogen adsorptive capacity which essentially increases the residence time in the catalyst bed for the average hydrogen molecule for a given mass flow rate.

Adsorption studies were performed in an effort to establish a relationship between physical adsorptive capacity and catalyst conversion activity and between chemisorptive capacity and catalyst conversion activity. Adsorption isotherms were constructed from experimental test data on two catalysts at 63.16°K, 77.0°K, 87.8°K, and 194.6°K. No appreciable chemisorption is assumed at these temperatures. A preliminary correlation derived from data on the hydrous ferric oxide gel catalyst showed that the ratio of relative adsorptive capacities and relative conversion activities at 77.0°K and 63.16°K were essentially equal. This suggests that the conversion activity is a direct function of the adsorptive capacity.

A mathematical expression for the process of conversion of ortho-to parahydrogen on a catalytic surface, which takes into account the preferential adsorption of orthohydrogen, was developed. Application of this expression to the analysis of dynamic conversion catalyst permits the evaluation of the separation factor of catalysts at a given temperature. The separation factor is defined as the ratio of concentrations of ortho- to parahydrogen in the adsorbed phase as compared to that in the gas phase. Theoretically, the separation factor increases as the temperature decreases and is considered essentially independent of the nature of the catalyst surface. Calculated values of the separation factor were in agreement with values determined at these temperatures by another method and reported by Sandler (2). These separation factors were also in agreement with the predicted temperature effect.

The apparatus for the study of the magnetic properties of the catalyst materials was set up and calibrated and the techniques for analyzing the magnetic data were established. Preliminary tests showed that many catalyst samples exhibit ferromagnetic character at cryogenic temperatures. Since evaluation of the magnetic moment is best performed in the temperature region where ferromagnetism is absent, the apparatus was modified for operation at ambient temperature and above to permit the determination of magnetic susceptibility at temperatures above the Curie temperature and subsequent calculation of the average magnetic moment per molecule of active specie in the advanced catalysts.

V. REFERENCES

1. Weitzel, D. H., et al, J. Res. Nat. Bur. Stand., 60, 231 (1958).
2. Sandler, Y. L., J. Phys. Chem. 58, 58 (1954).
3. Cunningham, C. M. and H. L. Johnston, J. Am. Chem. Soc. 80, 2377 (1958).
4. Taylor, H. S. and H. Diamond, J. Am. Chem. Soc. 55, 2613 (1933).
5. Taylor, H. S. and H. Diamond, J. Am. Chem. Soc. 57, 1251 (1935).
6. Farkas, L. and L. Sandler, J. Chem. Phys. 8, 248 (1940).
7. Turkevich, J. and P. Selwood, J. Am. Chem. Soc. 63, 1077 (1944).
8. Wigner, E., Z. Physik. Chem. B23, 28 (1933).
9. Kalckar, F. and E. Teller, Proc. Roy. Soc. A150, 530 (1935).
10. Farkas, L. and H. Sachsse, Z. Physik. Chem. B23, 1, 19 (1933).
11. Buyarnov, R. A., Kinetika i Kataliz Vol. 1, No. 4, Nov.-Dec. 1960.
12. Selwood, P. W., Magnetochemistry, Second Edition Interscience Publishers, Inc., New York, 1956, p. 149.
13. Weiss, P., J. Phys. 6, 661 (1907).
14. Bates, L. F., Modern Magnetism, Fourth Edition, Cambridge Univ. Press, p. 146 (1961).
15. Selwood, P. W., Magnetochemistry, Second Edition Interscience Publishers, Inc., New York, 1956, p. 159.

APPENDIX I

Derivation of Equation for Evaluating the Separation Factor of Catalysts

Assumptions

a. The ortho-parahydrogen conversion takes place only in the first adsorbed layer of the catalyst. The homogeneous conversion in gaseous hydrogen is slow and can be neglected.

b. There is a preferential adsorption of orthohydrogen by the surface. All hydrogen in the chamber except the first adsorbed layer is at the same ortho-parahydrogen concentration.

c. The conversion within the first adsorbed layer is first order and rate determining.

From these assumptions the following differential equation can be written.

$$-\frac{dC_g^o}{dt} = k_1 C_s^o - k_2 C_s^p \qquad (1)$$

where C_g^o = mole fraction of orthohydrogen in the main body of the gas at time t.

C_s^o = mole fraction of orthohydrogen on the surface at time t.

C_s^p = mole fraction of parahydrogen on the surface at time t.

k_1 = forward reaction rate constant.

k_2 = reverse reaction rate constant.

Defining the separation factor by

$$S = \frac{C_s^o / C_s^p}{C_g^o / C_g^p}$$

and noting that

$$C_s^o + C_s^p = 1$$

$$C_g^o + C_g^p = 1$$

Equation (1) becomes

$$-\frac{dC_g^o}{dt} = k_1 C_s^o - k_2 (1-C_s^o) \qquad (2)$$

and

$$S = \frac{C_s^o/(1-C_s^o)}{C_g^o/(1-C_g^o)} \qquad (3)$$

Letting $\frac{dC_g^o}{dt}$ in Equation (2) approach zero at infinite time

$$k_1 (C_s^o)^\infty = k_2 \left[1-(C_s^o)^\infty\right] \qquad (4)$$

where the superscript, ∞, denotes the equilibrium mole fraction of orthohydrogen at infinite time.

Combining Equation (3) and (4)

$$k_2 = \frac{k_1 S (C_g^o)^\infty}{1-(C_g^o)^\infty}$$

Let $\alpha = \frac{(C_g^o)^\infty}{1-(C_g^o)^\infty}$

then $k_2 = k_1 S \alpha$

From Equation (3)

$$C_s^{\,o} = \frac{S\,C_g^{\,o}}{C_g^{\,o}(S-1)+1}$$

Substituting k_2 and $C_s^{\,o}$ into Equation (2) and rearranging the following expression is obtained

$$\int_{C_i}^{C_o} \frac{C_g^{\,o}(S-1)+1}{C_g^{\,o} - (1-C_g^{\,o})}\, dC_g^{\,o} = -k_1 S \int_o^t dt \qquad (5)$$

where C_o = mole fraction of orthohydrogen in the main body of the gas at time t.

C_i = mole fraction of orthohydrogen in the main body of the gas at time o.

Performing the indicated integration by parts and rearranging, the following expression is obtained.

$$\ln \frac{\frac{C_e-C_i}{C_e-C_o}}{C_i-C_o} = k_1 S \frac{(1+\alpha)^2}{(S-1)\alpha+1+\alpha} \cdot \frac{t}{C_i-C_o} - \frac{(S-1)(1+\alpha)}{(S-1)\alpha+1+\alpha} \qquad (6)$$

Recalling that

$$\alpha = \frac{(C_g^{\,o})^{\infty}}{1-(C_g^{\,o})^{\infty}} \quad \text{or} \quad = \frac{C_e}{1-C_e}$$

where C_e = equilibrium mole fraction of orthohydrogen in the main body of the gas at infinite time

and substituting $\propto$ into Equation (6)

$$\ln \frac{C_e - C_i}{C_e - C_o} = \frac{k_1 S}{(1-C_e)\ 1 + (S-1)\ C_e} \cdot \frac{t}{C_i - C_o} - \frac{S-1}{1 + (S+1)\ C_e} \qquad (7)$$

The log mean concentration driving force is defined by

$$LMDF = \frac{C_i - C_o}{\ln \frac{C_e - C_i}{C_e - C_o}}$$

For a flow system the time interval, t, over which the conversion takes place is given by

$$t = \frac{V_R}{V}$$

where V_R = volume of catalyst chamber, ft^3

V = volumetric flow rate, $\frac{ft^3}{min}$

Making the above substitutions into Equation (7), the following equation is finally obtained. This equation appears in section III-F.

$$\frac{1}{LMDF} \quad \frac{k_1 S\ V_R}{(1-C_e)\ 1 + (S-1)\ C_e} \quad \frac{1}{V\ (C_i - C_o)} \quad \frac{S-1}{1 + (S-1)\ C_e}$$

Summary of Nomenclature

C_e = equilibrium mole fraction of orthohydrogen in the main body of the gas at infinite time.

C_i = mole fraction of orthohydrogen in the gas entering the catalyst chamber.

C_o = mole fraction of orthohydrogen in the gas leaving the catalyst chamber.

k_1 = forward reaction rate constant, min^{-1}.

LMDF = log mean concentration driving force.

S = separation factor.

V = volumetric flow rate of hydrogen, ft^3/min.

V_R = volume of catalyst chamber, ft^3.

UNCLASSIFIED